




# Facile preparation of magnetite–cellulose nanocomposite from a sustainable resource

KEBEDE GAMO SEBEHANIE<sup>1,2</sup>, SURAFEL SHIFERAW LEGESE<sup>3</sup>,  
ALBERTO VELÁZQUEZ DEL ROSARIO<sup>4</sup>, ABUBEKER YIMAM ALI<sup>5</sup>  
and FEMI EMMANUEL OLU<sup>2,\*</sup> 

<sup>1</sup>Bio and Emerging Technology Institute, Nanotechnology Directorate, P.O. Box 5954, Addis Ababa, Ethiopia

<sup>2</sup>Faculty of Materials Science and Engineering, JiT, Jimma University, P.O. Box 378, Jimma, Ethiopia

<sup>3</sup>Interdisciplinary Centre for Energy Research, Indian Institute of Science, Bangalore 560012, India

<sup>4</sup>Federal Technical and Vocational Education and Training Institute, P.O. Box 190310, Addis Ababa, Ethiopia

<sup>5</sup>School of Chemical and Bio Engineering, AAiT, Addis Ababa University, P.O. Box 1176, Addis Ababa, Ethiopia

\*Author for correspondence (foluemm@gmail.com)

MS received 2 June 2022; accepted 17 September 2022

**Abstract.** Because of the synergistic effect of the individual nanomaterials, nanocomposites are becoming an important class of materials, allowing the creation of end-products with different properties and greater performance than when used individually. This study aims to create magnetite nanoparticles (MNPs) from iron ore and nanocellulose fibre (CNF) from sugar bagasse to make magnetite–cellulose nanocomposites. X-ray diffraction and Fourier-transform infrared spectroscopy were used to confirm the prepared nanomaterials, and scanning electron microscopy was used to investigate the morphology of the nanomaterials. The nanocomposites were created using two methods: (1) adding CNF before the MNPs precipitated and (2) adding CNF after the MNPs precipitated. There was a difference in crystallite size, with the smallest being 23 nm for the one prepared before precipitation and 31 nm for pure MNPs. The magnetic properties of the as-prepared nanomaterials were also investigated using the vibrating sample magnetometer technique. MNPs and MNPs–CNF nanocomposites have superparamagnetic properties, with nearly zero coercivity for all samples and saturation magnetizations of 42.8, 30.7, and 23.2 emu g<sup>-1</sup> for pure MNPs, MNPs–CNF (before precipitation) and MNPs–CNF (after precipitation), respectively. Thermogravimetric analysis was used to investigate the thermal behaviour of the nanocomposite. The incorporation of cellulose nanofibre prevented aggregation while having a negligible effect on thermal stability.

**Keywords.** Magnetite nanoparticles; nanocellulose fibre; sugarcane bagasse.

## 1. Introduction

The search for new materials for different technological applications is the focus of many researchers. Nowadays, nanomaterials are becoming the best solution for many global challenges. However, despite its numerous advantages, environmental and health issue is still a question for many peoples. Furthermore, some applications, such as wastewater treatment, require a significant amount of nanomaterials. Therefore, we have to look for nanomaterials that are both feasible and non-toxic.

Magnetite minerals are mainly used to extract iron for the production of steel. However, when the size of magnetite is at the nanoscale, it has many technological benefits [1]. In recent decades, comprehensive investigations and developments have been observed in nano-sized magnetite particles. Moreover, their biocompatibility, non-toxicity, superparamagnetic, high surface area and environmentally

friendly behaviour of magnetite nanoparticles (MNPs) [2] make them ideal for novel applications, including biomedical, catalysis, information storage and wastewater treatment [3].

Since pure magnetite has some drawbacks like agglomeration and low stability [4], it is not easy to use for the required purpose. Therefore, to overcome these problems, surface modification of the pure MNPs with organic and inorganic materials has been the best solution [5]. Moreover, when the surface is modified, it (1) prevents oxidizing efficiently, (2) will decrease agglomeration and (3) will have the possibility to functionalize with other materials to use it for a specific purpose [5].

Magnetic nanoparticles (MNPs) can be combined with different materials, creating final products with features other than magnetic properties [6,7]. Compounds that include MNPs and cellulose have attracted much interest due to the effect of synergy taken from each section, which

will have an advantage in creating new materials, such as magnetized cellulose, that we would not be able to obtain if we used the MNPs and cellulose materials separately [8–10]. This hybrid material can show different textures and functional properties, as it also represents a new concept with benefits such as biocompatibility and biodegradability [11–15]. Several applications can be considered for cellulose–MNP building materials, such as nanocatalysts for removal of textile dyes [16], conductive paper [17], transparent magneto-optical films applications [18], and catalytic and antibacterial works [19].

Because cellulose is a major component of all plant structures [20], we may classify it as a sustainable resource. Due to its hydrophilic nature, stereoregularity and poly-functionality, cellulose's chemical structure differs from many synthetic polymers [21]. In addition, its biodegradability, non-toxicity, low density, availability and combined with its inexpensive cost, this natural biopolymer material has attracted the interest of many researchers. However, to be used for many advanced technological applications, the cellulose materials must be at the micro or nanoscale and can be modified for the intended function [22]. Furthermore, nanocellulose has surprising features like high mechanical strength, thermal stability, high surface area and aspect ratio, tailorability of the surface chemistry, and interesting optical and rheological properties [23,24]. These properties of nanocellulose make them an ideal green nanomaterial to this day.

Furlan *et al* [25] reported preparing magnetite–cellulose hybrid film using the casting method; the Sisal plant was used as the source and LiCl/DMAc as the solvent system for the cellulose. Magnetizations of the film range from (23–37) emu g<sup>-1</sup> at 300 K for different MNPs and a superparamagnetic behaviour at room temperature. Chen *et al* [26] studied CNCs magnetized with the decoration of iron oxide nanoparticles (IONPs) prepared by the thermal decomposition process of iron carbonyl precursors on the surface of CNCs, IONPs consisting of mixtures of Fe<sub>3</sub>O<sub>4</sub> and Fe<sub>2</sub>O<sub>3</sub> with an average diameter of 20 nm were attached to the CNCs. Likewise, Small and Johnshon [27] fabricated hybrid materials of magnetic nanoparticles and cellulose fibres by coating bleached kraft fibres (*Pinus radiata*) without changing the inherent properties of the fibre, such as tensile strength and flexibility. The saturation magnetization ranges from 62 to 70 emu g<sup>-1</sup>, with coercive fields in the range of 19–122 Oe.

Different researchers investigated magnetite–cellulose nanocomposite for environmental remediation applications. For instance, Carvalho Costa [28] prepared magnetized coconut fibres from agro-industrial waste using MNPs by a co-precipitation reaction in alkaline media to apply for Cr(VI) adsorption. Liu *et al* [29] reported magnetite cellulose–chitosan hydrogels prepared from ionic liquids to remove heavy metal ions (Cu<sup>2+</sup>, Fe<sup>2+</sup> and Pb<sup>2+</sup>). Also, Elrhman [30] synthesized core–shell MNPs with modified nanocellulose to remove radioactive ions (<sup>228</sup>Ac, <sup>212</sup>Pb,

<sup>212</sup>Bi and <sup>208</sup>Tl) from an aqueous solution. The best adsorption capacity was observed for Fe<sub>3</sub>O<sub>4</sub>@ nano-cellulose citrate.

The chemical co-precipitation method was used to synthesize magnetic composite nanoparticles (MNPs), and this was achieved by surface anchoring of iron oxide (Fe<sub>3</sub>O<sub>4</sub>) on carboxyl cellulose nanospheres as reported by Qin *et al* [16]. The removal efficiency for navy blue was 90.6% at the first minute of the degradation reaction and 98.0% for 5 min at a weight ratio of cellulose to iron of 1:2. Amiralian *et al* [31], in their work, prepared magnetic nanocellulose membranes for the application of Rhodamine B, removal of a common hydrophilic organic dye applied in industry. The cellulose nanofibres were used as a template to synthesize magnetic nanoparticles with a diameter below 20 nm. The Fe<sub>3</sub>O<sub>4</sub> nanoparticles coated on the cellulose nanofibres possess a very high saturation magnetization (67.4–38.5 emu g<sup>-1</sup>) due to the crystallite size of the nanoparticles.

Besides, for versatile application, El-Nahas *et al* [32] used functionalized cellulose–magnetite nanocomposite for biodiesel production using rice straw as a nanocellulose source, and the sulphonated cellulose–magnetite nanocomposite (MSNC) showed a high catalytic activity towards the esterification reaction (96%), which resulted from the impregnation of magnetite (0.98 wt%). Galateanu *et al* [33] synthesized bacterial cellulose and magnetic nanoparticle nanocomposites to heal chronic wounds. Li *et al* [34] fabricated uniform, flexible and transparent magnetic nanopaper using magnetite nanoparticle immobilization on cellulose nanofibre networks. Xiong *et al* [19] prepared Fe<sub>3</sub>O<sub>4</sub>/Ag@ nano-fibrillated cellulose nanocomposites aerogel and film to apply for catalysis and antibacterial agent.

Some research has been done on using magnetized nanocellulose for different technological applications. However, the magnetite nanoparticle source is mainly from a chemical precursor, which is not applicable for applications that need significant MNPs like wastewater treatment. To the best of our knowledge, no research on magnetite–cellulose nanocomposites using both natural resources as starting ingredients has been published.

This study synthesized nanocellulose fibre from sugarcane bagasse and MNPs from iron ore. Then the fabrication of magnetite–cellulose nanocomposites using two easy approaches was carried out. Finally, the crystalline nature and the magnetic properties of the synthesized nanomaterials was investigated.

## 2. Experimental

### 2.1 Raw materials and reagents

Iron ore and sugarcane bagasse are the primary raw materials. The following chemicals were used for the

extraction and synthesis of both MNPs and cellulose nanofibre (CNF): hydrochloric acid, sodium hydroxide, hydrogen peroxide, tri-butyl phosphate, heptanol, formic acid, sulphuric acid ( $\text{H}_2\text{SO}_4$ ), sodium chlorite ( $\text{NaClO}_2$ ), and glacial acetic acid. All were of analytical grade, purchased from Loba Chemie Pvt. Ltd, Mumbai, India. Sodium borohydride, the analytical grade, was purchased from Scientific Laboratory Supplies Ltd., England. 2-Ethyl-hexanol and sodium hypochlorite ( $\text{NaClO}$ ) were of analytical grade and purchased from Unichem Laboratories, India.

## 2.2 Experimental methods

**2.2a Synthesis of MNPs:** A similar procedure was followed to synthesize MNPs with a slight modification to our previously published article [35]. In detail, 60 g of iron ore powder and 90 ml of HCl were mixed in a beaker and stirred at  $80^\circ\text{C}$  for 3 h. The leachate was centrifuged and discarding the residue, then 80 ml of 30%  $\text{H}_2\text{O}_2$  was added as an oxidant to 60 ml of the obtained supernatant, such that all  $\text{Fe}^{2+}$  ions were oxidized to  $\text{Fe}^{3+}$  ions. To selectively extract  $\text{Fe}^{3+}$  from the leachate, 50 ml of an aqueous solution of the leachate was mixed with 50 ml of a solvent extractant containing (34 ml of TBP, 10 ml of 2-ethyl-hexanol and 6 ml of heptanol) in a separating funnel. The mixture was stirred for 10 min to maintain uniformity and left for 10 min to separate the organic and aqueous phases. Finally, the aqueous solution was centrifuged at 3000 rpm for 10 min to remove the silica particles that were not dissolved during the digestion process using HCl.

The stripping step was carried out by mixing 50 ml of distilled water with 25 ml of the iron-extractant complex, with the volume ratio of the iron-extractant complex to the aqueous solution retained at 1:2. The mixture was vigorously stirred for 20 min before being placed in a separatory funnel for 10 min to reach phase separation. Then, the aqueous phase was separately collected to obtain a pure  $\text{Fe}^{3+}$  solution.

To synthesize MNPs, aqueous co-precipitation of  $\text{Fe}^{3+}$  and  $\text{Fe}^{2+}$  at a ratio of 2:1 was carried out in the presence of a base (pH 9–12). Then, 18 ml of  $\text{NaBH}_4$  (0.033 wt%) aqueous solution was added to 60 ml of  $\text{Fe}^{3+}$  aqueous solution to reduce to  $\text{Fe}^{2+}$  and stirred for 10 min. Finally, 200 ml of 2M NaOH alkaline solution was gradually added to 200 ml of iron aqueous solution (106 ml  $\text{Fe}^{3+}$  aqueous solution, 70 ml  $\text{Fe}^{2+}$  aqueous solution and 24 ml distilled water). Finally, the mixed solution was stirred for 10 min at  $40^\circ\text{C}$ . Before collecting the nanoparticles with a bar magnet, they were washed three times with distilled water.

**2.2b Synthesis of nanocellulose from bagasse:** Before chemical pretreatment, the bagasse was cleaned by washing it with water several times and dried. Then the dried bagasse was grounded to make a fine powder. Finally, the powdered bagasse was ready for purification and chemical

treatment to isolate cellulose nanofibre (CNF). Then the nanocellulose fibre extraction was carried out according to the methods described elsewhere with slight modifications [36].

First, the powdered bagasse was treated with 10% NaOH (1:10 (w/v); dry bagasse to alkaline solution ratio) in a 3-l flask in a water bath at  $90^\circ\text{C}$  for 1.5 h. Next, the residue of the bagasse powder was filtered and washed continuously with hot distilled water. Then the pulps were further treated with a mixture of 20% formic acid, 20% acetic acid and 7.5%  $\text{H}_2\text{O}_2$  (2:1:2) solution (1:10 solid to liquid ratio) in the water bath at  $90^\circ\text{C}$  for 1.5 h. Next, the de-lignified bagasse was filtered to separate the cooking liquor (which contains lignin and hemicellulose) from cellulose and washed with hot water. Finally, bleaching was carried out by treating the pulps with 7.5%  $\text{H}_2\text{O}_2$  in 4% NaOH solution (1:10 fibre to liquid ratio), first at room temperature for 30 min, then on a water bath at  $70^\circ\text{C}$  for 30 min. The pulp is then rinsed repeatedly with hot water filtered to remove the remaining lignin and dried in an oven at  $60^\circ\text{C}$  until getting a constant weight [36].

As a final stage, the dried powders were slowly added into the  $\text{H}_2\text{SO}_4$  solution (63% w/v) (1:3 v/w solid to liquid ratio) under vigorous stirring at room temperature for 1 h. Then ice water was added to the mixture to quench the hydrolysis. Then the mixture was centrifuged at 1000 rpm for 10 min and then at 10,000 rpm for 15 min to obtain CNF. Next, the CNF was washed and centrifuged repeatedly (3 times) before dialysis against distilled water for 2 days. After that, the CNF suspension was sonicated for a few minutes, filtered, and finally dried in an oven at  $40^\circ\text{C}$  overnight to get fine white powder.

**2.2c Synthesis of magnetite–cellulose nanocomposite:** Two approaches were followed to investigate the effect and compare the synthesized magnetite–cellulose nanocomposite. The first method was putting the cellulose nanofibre powder before the MNPs precipitate. The second approach was putting the cellulose nanofibre powder after the MNPs precipitate.

In detail, we add 2 g of nanocellulose powder in ferric and ferrous solution, stirring it at a temperature of  $60^\circ\text{C}$  for about 30 min and then gradually adding the NaOH. Then the black precipitate will be formed and washed with deionized water to remove impurities and pure nanocellulose as much as possible.

## 3. Result and discussion

X-ray diffraction (XRD) was used to investigate the crystalline nature, phases and crystallite size of the synthesized cellulose nanofibre (CNF), MNPs and magnetite–cellulose nanocomposite (figure 1). For pure cellulose nanofibre, we see the characteristic peaks at  $2\theta = 14.9^\circ$  and  $22.9^\circ$ , which correspond to the crystal planes of (101) and (002),

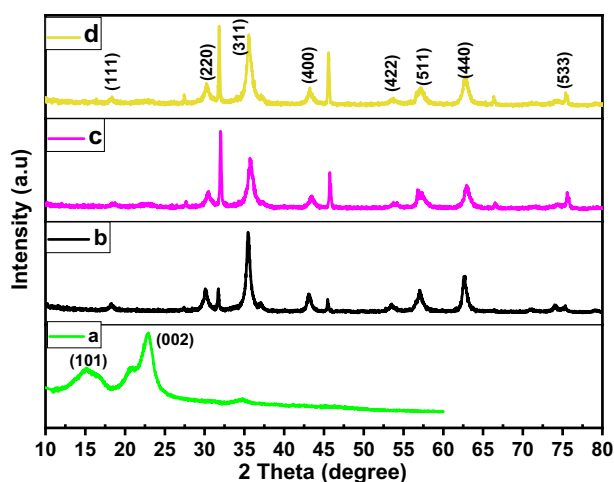


**Figure 1.** XRD patterns for (a) pure nanocellulose fibre, (b) pure MNPs, (c) MNPs–CNF (before precipitation) and (d) MNPs–CNF (after precipitation).

respectively [37]. And for pure MNPs, the characteristic peaks formed at  $2\theta = 18.3, 30.1, 35.5, 43.1, 53.5, 57, 62.6$  and  $75.4$ , which correspond to the crystal planes of (111), (220), (311), (400), (422), (511), (440) and (533), respectively. However, there are peaks around  $2\theta = 31.7$  and  $45.6$ , which may have arisen due to impurities found or the coexistence of other forms of iron oxides like hematite or maghemite. The MNPs have an inverse cubic spinel structure [38].

For the magnetite–cellulose nanocomposite, we see an additional diffraction peak at  $2\theta = 15.9, 22.6$ , which is related to the cellulose nanofibre and confirms that magnetite nanoparticle is on the surface of the cellulose nanofibre. When we compare the phases present and the diffraction pattern in both the magnetite–cellulose nanocomposite before and after, they are almost the same, which tells us there is no effect on the phases and the crystalline nature of the nanocomposite whether we put the nanocellulose powder before precipitation or after precipitation. However, according to the Debye–Scherrer formula, the average crystallite size for a composite prepared before the MNPs precipitate is 23 nm, while a composite prepared after the magnetite nanoparticle precipitate has an average crystallite size of 26 nm. The pure MNPs have a larger average crystallite size of 31 nm (almost similar average crystallite size with the previously published article [35]) than the composites, which may be due to the addition of nanocellulose fibre affecting the nucleation and growth process. Figure 2 shows the comparison of the diffraction patterns for MNPs synthesized from the ore and chemical precursor. We can see that they have almost the same pattern except for the iron ore source at around  $2\theta = 31.7$ . They have an additional peak, which could be due to impurities.

Figure 3 shows the Fourier-transform infrared (FTIR) spectra of pure cellulose nanofibre, pure MNPs and

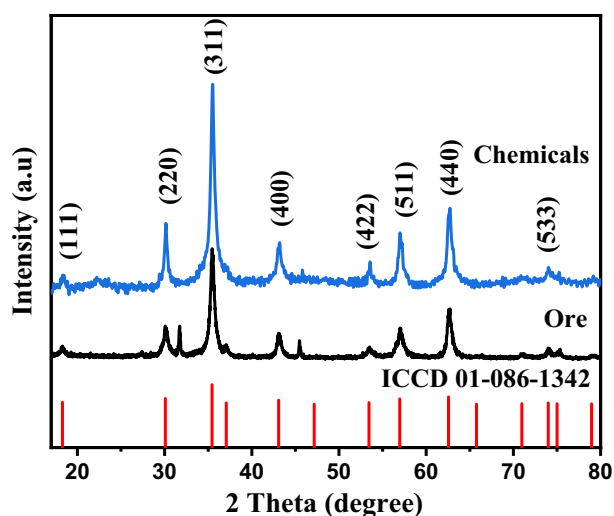


**Figure 2.** XRD patterns for MNPs prepared from the iron ore and chemical precursor.

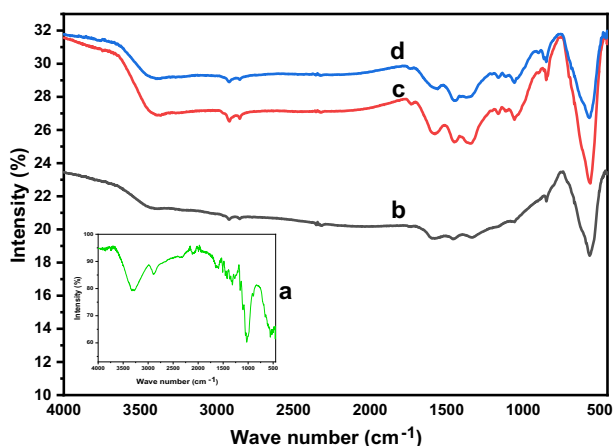


**Figure 3.** FT-IR spectra for (a) pure CNF, (b) pure MNPs, (c) MNPs–CNF (before the precipitation), (d) MNPs–CNF (after the precipitation).

magnetite–cellulose nanocomposite. For cellulose nanofibre (figure 3a), the broad peak around  $3333\text{ cm}^{-1}$  is attributed to the O–H stretching vibration of the OH group [30]. The absorption peak around  $2893\text{ cm}^{-1}$  is due to the C–H stretching vibration [38]. The peak at  $1639\text{ cm}^{-1}$  was the O–H bending of adsorbed water [39]. The band at around  $1432\text{ cm}^{-1}$  was ascribed to C–O–H stretching vibration, and around  $1317\text{ cm}^{-1}$  assigned to  $\text{CH}_2$  wagging. The vibration of C–O–C in the pyranose ring is indicated by the absorption peak at  $1031\text{ cm}^{-1}$ , referring to the structure of cellulose/lignin. After the chemical treatment process, the cellulose samples did not have a peak at  $1728\text{ cm}^{-1}$ , indicating that lignin and hemicellulose were removed from sugarcane bagasse. For pure MNPs (figure 3b), the band at  $569\text{ cm}^{-1}$  corresponds to the vibration of the Fe–O bonds. The broad absorption peaks around  $3428$  and  $1618\text{ cm}^{-1}$  correspond to O–H molecules' stretching and bending,

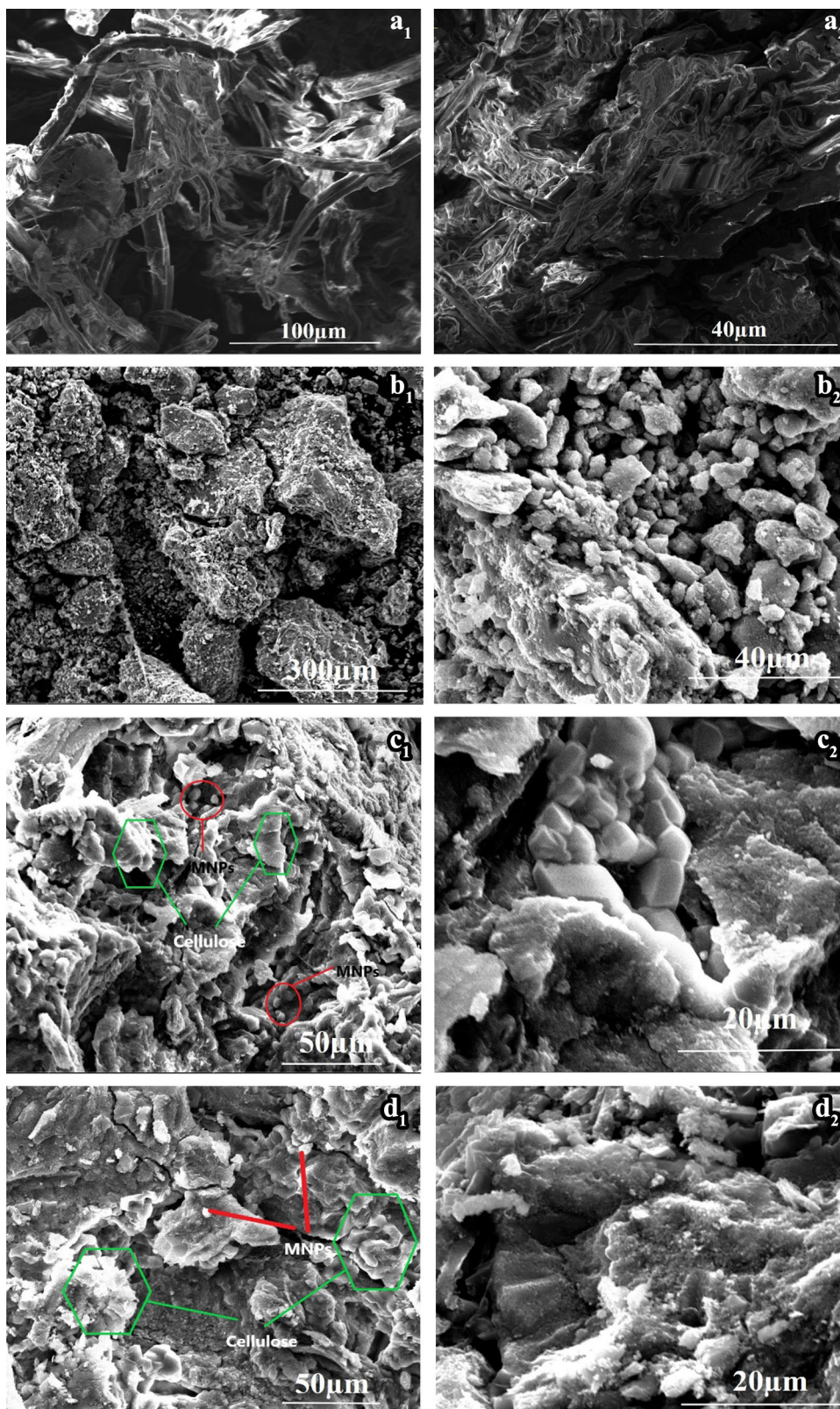


**Figure 4.** Scanning electron microscopy images at different magnifications for (a<sub>1</sub> and a<sub>2</sub>) pure CNF, (b<sub>1</sub> and b<sub>2</sub>) pure MNPs, (c<sub>1</sub> and c<sub>2</sub>) MNPs–CNF before precipitation and (d<sub>1</sub> and d<sub>2</sub>) MNPs–CNF after precipitation.

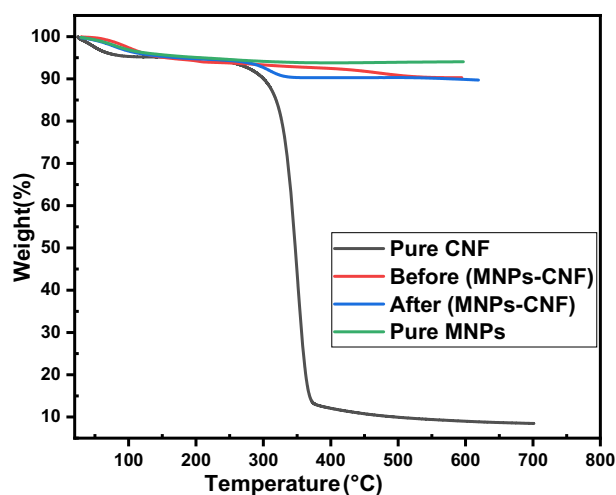


**Figure 5.** Thermogravimetric analysis of the synthesized nanomaterials and nanocomposites.

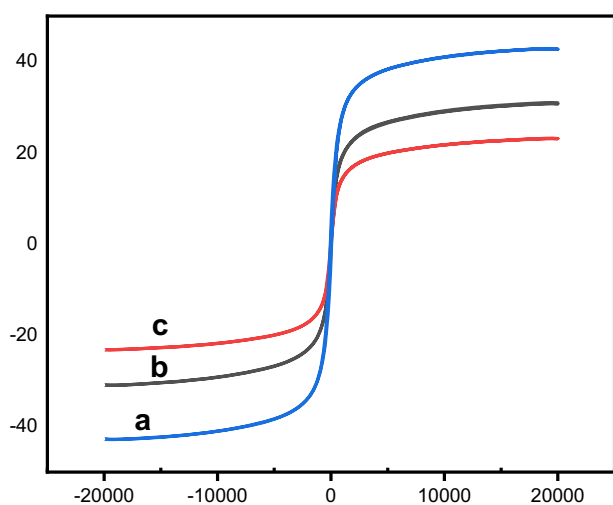


**Figure 6.** Vibrating sample magnetometer hysteresis loop for (a) pure MNPs, (b) MNPs–CNF (before the precipitation) and (c) MNPs–CNF (after the precipitation).

respectively [40]. The prepared magnetite–cellulose nanocomposite before (figure 3c) and after (figure 3d) exhibited similar characteristic peaks. Magnetite–cellulose nanocomposite showed a non-symmetric phase ring peak around  $111\text{ cm}^{-1}$ , non-symmetric out-of-phase ring at  $847\text{ cm}^{-1}$  and skeletal vibrations acyl group C–O at  $1059\text{ cm}^{-1}$ , that is, the characteristics of cellulose ring. For magnetite–cellulose nanocomposite, the peak at  $1456\text{ cm}^{-1}$  disappeared, and the peak at  $1450\text{ cm}^{-1}$  was observed. This result also showed that the cellulose crystalline form of magnetite–cellulose nanocomposite changed from cellulose (I) to cellulose (II) (Colom and Carrillo [41]).

We used scanning electron microscopy to observe the morphology of cellulose fibre, pure magnetite nanoparticle and magnetite–cellulose nanocomposite. For pure nanocellulose fibre the surface is smooth (figure 4a1, a2) and

estimated to be a few micrometres in length. For pure MNPs (figure 4b1, b2), since one of the main challenges for MNPs is aggregation due to high surface energy, it is very difficult to observe individual particle size; however it is conventionally expected based on the synthesis route and our previous report that the estimated size of the as-synthesized magnetite particle is in the nanometre range. For magnetite–cellulose nanocomposite (figure 4c, d), the morphology of the cellulose fibre surface have irregular shape and crinkled, and most of the MNPs are probably covered by the cellulose fibre.

Thermal properties of cellulose nanofibre, pure MNPs and magnetite–cellulose nanocomposite were analysed using thermogravimetric analysis, shown in figure 5. For the CNFs, the initial weight loss (4.8%) at the temperature below  $115^\circ\text{C}$  refers to the evaporation of adsorbed water. Then a plateau appears before  $266^\circ\text{C}$ . Then a significant weight loss (80%) at temperatures between 266 and  $371^\circ\text{C}$  was observed due to the degradation of cellulose nanofibre; finally, slow decomposition at temperatures between 371 and  $700^\circ\text{C}$  and a weight loss of 6%. CNF of 90.8% was thermally oxidized under air, leaving around 9% ash residue [42]. The weight loss of pure MNPs was about 4% below  $120^\circ\text{C}$ , primarily to water molecule evaporation. The weight loss (3%) during the temperature ranges of  $120\text{--}420^\circ\text{C}$  and up to  $440^\circ\text{C}$  was caused by the degradation of the agent's physisorption and chemisorption at the surface of the MNPs, respectively. The minor weight increase at  $420^\circ\text{C}$  is due to the transition of magnetite to hematite [43]. The thermal behaviour of the magnetite–cellulose nanocomposite is similar to that of pure magnetite. The incorporation of MNPs affects the thermal decomposition of nanocellulose, as multiple stages of degradation were absent from the thermogravimetric analysis curves. It is shown that the degradation of the CNFs was efficiently reduced when a magnetic layer was coated on the surface of CNFs, as shown in figure 5. It is worth pointing out that it is usually believed that metal oxides would promote the decomposition of organic products. No significant difference was observed for magnetite–cellulose nanocomposite prepared for adding cellulose nanofibre before and after the MNPs precipitate.

The magnetic property of the synthesized pure MNPs and nanocomposites were characterized using vibrating sample magnetometer, shown in figure 6. For pure MNPs, the saturation magnetization at room temperature was  $42.8\text{ emu g}^{-1}$ . For the nanocomposites, the saturation magnetization is 30.7 and 23.2 before and after the precipitation of the MNPs, respectively. As expected, the magnetite–cellulose nanocomposite has less magnetic saturation due to the cellulose, which may decrease its  $M_s$ . The remnant magnetization is 3.6 for pure MNPs and 1.08 for both nanocomposites before and after. The coercivity is almost zero indicating superparamagnetic property for all of the samples.

#### 4. Conclusion

Iron ore was used as a starting material; MNPs were successfully synthesized using the solvent extraction and co-precipitation method. Then, nanocellulose fibre was extracted from sugarcane bagasse using alkali treatment and acid hydrolysis. Finally, the nanocomposite from MNPs and nanocellulose fibre was prepared. The synthesized nanomaterials were characterized by XRD, scanning electron microscopy, FT-IR, thermogravimetric analysis and vibrating sample magnetometer, and we concluded that;

1. XRD and FT-IR confirmed the synthesized nanomaterials. Furthermore, they have similar characteristics to different kinds of reports in the literature.
2. The MNPs are superparamagnetic with saturation magnetization of 42.8, 30.7 and 23.2 emu g<sup>-1</sup> for pure MNPs, before precipitation and after precipitation. And almost zero coercivity for all the samples.
3. The nanocomposite preparation method (before and after the MNPs precipitate) affects the magnetic properties. The one prepared before the MNPs precipitate shows a large saturation magnetization of 30.7 emu g<sup>-1</sup> than the other (23.2).
4. When we compare the nanomaterials' crystallite size, the one prepared before the precipitation has the smallest crystallite and the pure MNPs have the largest crystallite size. This may be the result of the addition of nanocellulose to prevent agglomeration.
5. The synthesized nanomaterials can be a potential candidate for wastewater treatment, as after treatment of wastewater, using the advantage of magnetized cellulose, it can be easily separated from the treated water.

#### Acknowledgements

We would like to thank the Department of Materials Engineering at the Indian Institute of Science, Bangalore, India, for the magnetic measurement and other characterization. Thanks to the Bio and Emerging Technology Institute, Addis Ababa, Ethiopia, for financial support; Addis Ababa University, Chemistry Department, for allowing laboratory facility and Jimma University, Addis Ababa Science and Technology University.

#### References

- [1] Niculescu A G, Chircov C and Grumezescu A M 2021 *Methods* **199** 16
- [2] Novoselova L Y 2021 *Appl. Surf. Sci.* **539** 148275
- [3] Schwaminger S P, Syhr C and Berensmeier S 2020 *Crystals* **10** 214
- [4] Schwaminger S P, Bauer D, Fraga-García P, Wagner F E and Berensmeier S 2017 *Cryst. Eng. Commun.* **19** 246
- [5] Oguz M, Bhatti A A and Yilmaz M 2020 *Mater. Lett.* **267** 127548
- [6] Aguilera L S, Marcal R L S B, Campos J B, Silva M H P and Figueiredo AB-HS 2018 *J. Mater. Res. Technol.* **7** 350
- [7] Sanchez P A, Gundermann T, Dobroserdova A, Kantorovich S S and Odenbach S 2018 *Soft Matter* **14** 2170
- [8] El Khames Saad M, Khiari R, Elaloui E and Moussaoui Y 2014 *Arab. J. Chem.* **7** 109
- [9] Khiari R, Dridi-Dhaouadi S, Aguir C and Mhenni M F 2010 *J. Environ. Sci.* **22** 1539
- [10] Ali I and Gupta V K 2006 *Nat. Protoc.* **1** 2661
- [11] Liu S, Zhou J, Zhang L, Guan J and Wang J 2006 *Macromol. Rap. Commun.* **27** 2084
- [12] Zhou J, Li R, Liu S, Li Q, Zhang L, Zhang L *et al* 2008 *J. Appl. Polym. Sci.* **111** 2477
- [13] Liu S, Zhou J and Zhang L 2011 *Cellulose* **18** 663
- [14] Wang F, Yang Y, Ling Y, Liu J, Cai X, Zhou X *et al* 2017 *Biomaterials* **128** 84
- [15] Spiridonov V V, Panova I G, Makarova L A, Afanasov M I, Zezin S B, Sybachin A V *et al* 2017 *Carbohydr. Polym.* **177** 269
- [16] Qin Y, Qin Z, Liu Y, Cheng M, Qian P, Wang Q *et al* 2015 *Appl. Surf. Sci.* **357** 2103
- [17] Liu K, Nasrallah J, Chen L, Huang L and Ni Y 2015 *Carbohydr. Polym.* **126** 175
- [18] Li Y, Zhu H, Gu H, Dai H, Fang Z, Weadock N J *et al* 2013 *J. Mater. Chem. A* **1** 15278
- [19] Xiong R, Lu C, Wang Y, Zhou Z and Zhang X 2013 *J. Mater. Chem. A* **1** 14910
- [20] Olivera S, Muralidhara H B, Venkatesh K, Guna V K, Gopalakrishna K and Kumar K Y 2016 *Carbohydr. Polym.* **153** 600
- [21] Klemm D, Heublein B, Fink H-P and Bohn A 2005 *Angew. Chem. Int. Ed. English* **44** 3358
- [22] Phinichka N and Kaentling S 2018 *J. Mater. Res. Technol.* **7** 55
- [23] Barbash V, Yashchenko O and Kedrovskaya A 2017 *JSRR* **16** 1
- [24] Daud J B and Lee K-Y 2017 *Handb. Nanocellulose Cellulose Nanocompos.* **1** 101
- [25] Furlan D M, Morgado D L, de Oliveira A J A, Faceto A D, de Moraes D A, Varanda L C *et al* 2019 *J. Mater. Res. Technol.* **8** 2170
- [26] Chen L, Sharma S, Darienzo R E and Tannenbaum R 2020 *Mater. Res. Express* **7** 055003
- [27] Small A C and Johnston J H 2009 *J. Colloid Interface Sci.* **331** 122
- [28] Carvalho Costa A W M, Guerhardt F, Ribeiro Júnior S E R, Cãnovas G, Vanale R M, de Freitas Coelho D *et al* 2020 *Environ. Technol.* **42** 3595
- [29] Liu Z, Wang H, Liu C, Jiang Y, Yu G, Mu X *et al* 2012 *Chem. Commun.* **48** 7350
- [30] Elrhman H M A 2020 *Results Mater.* **8** 100138
- [31] Amiralian N, Mustapic M, Hossain Md S A, Wang C, Konarova M, Tang J *et al* 2020 *J. Hazard. Mater.* **394** 122571
- [32] El-Nahas A M, Salaheldin T A, Zaki T, El-Maghrabi H H, Marie A M, Morsy S M *et al* 2017 *Chem. Eng. J.* **322** 167
- [33] Galateanu B, Bunea M-C, Stanescu P, Vasile E, Casarica A, Iovu H *et al* 2015 *Stem Cells Int.* <https://doi.org/10.1155/2015/195096>
- [34] Li Y, Zhu H and Gu H 2013 *J. Mater. Chem. A* **1** 15278

- [35] Sebehanie K G, Femi O E, Del Rosario V and Ali A Y 2020 *Mater. Res. Express* **7** 105016
- [36] Sun J X, Sun X F, Zhao H and Sun R C 2004 *Polym. Degrad. Stab.* **84** 331
- [37] Johar N, Ahmad I and Dufresne A 2012 *Ind. Crop. Prod.* **37** 93
- [38] Khalil H P S A, Ismail H, Rozman H D and Ahmad M N 2001 *Eur. Polym. J.* **37** 1037
- [39] Le Troedec M, Sedan D, Peyratout C, Bonnet J P, Smith A, Guinebretiere R *et al* 2008 *Appl. Sci. Manuf.* **39** 514
- [40] Ebrahiminezhad A, Ghasemi Y, Rasoul-Amini S, Barar J and Davaran S 2012 *Bull. Korean Chem. Soc.* **33** 3957
- [41] Colom X, Carrillo F 2002 *Eur. Polym. J.* **38**(11) 2225
- [42] Cheng M, Qin Z, Liu Y, Qin Y, Li T, Chen L *et al* 2014 *J. Mater. Chem. A* **2** 251
- [43] Petcharoen K and Sirivat A 2012 *Mater. Sci. Eng. B* **177** 421